

Identification of a Minimal Core of the Synaptic SNARE Complex Sufficient for Reversible Assembly and Disassembly[†]

Dirk Fasshauer,[‡] William K. Eliason,[§] Axel T. Brünger,[§] and Reinhard Jahn^{*:‡}

Department of Neurobiology, Max-Planck-Institute for Biophysical Chemistry, D-37077 Göttingen, Germany, and Howard Hughes Medical Institute and Department of Molecular Biochemistry and Biophysics, Yale University, New Haven, Connecticut 06510

Received March 10, 1998; Revised Manuscript Received May 8, 1998

ABSTRACT: Assembly of the three neuronal membrane proteins synaptobrevin, syntaxin, and SNAP-25 is thought to be one of the key steps in mediating exocytosis of synaptic vesicles. *In vivo* and *in vitro*, these proteins form a tight complex. Assembly is associated with a large increase in α -helical content, suggesting that major structural and conformational changes are associated with the assembly reaction. Limited proteolysis by trypsin, chymotrypsin, and proteinase K of the ternary complex formed from recombinant proteins lacking their membrane anchors revealed a SDS-resistant minimal core. The components of this core complex were purified and characterized by N-terminal sequencing and mass spectrometry. They include a slightly shortened synaptobrevin fragment, C- and N-terminal fragments of SNAP-25, and a C-terminal fragment of syntaxin that is slightly larger than the previously characterized H3 domain. Recombinant proteins corresponding to these fragments are sufficient for assembly and disassembly. In addition, each of the two SNAP-25 fragments can individually form complexes with syntaxin and synaptobrevin, suggesting that they both contribute to the assembly of the SNARE complex. Upon complex assembly, a large increase in α -helical content is observed along with a significantly increased melting temperature (T_m). Like the full-length complex, the minimal complex tends to form an oligomeric species; global analysis of equilibrium ultracentrifugation data suggests a monomer–trimer equilibrium exists. These conserved biophysical properties may thus be of fundamental importance in the mechanism of membrane fusion.

Exocytosis is a basic feature of every eukaryotic cell. It involves the attachment of a transport vesicle at the plasma membrane (also referred to as docking) and subsequently the fusion of the two participating bilayer membranes. Although lipid bilayers can be fused artificially in the test tube by perturbing the microenvironment of the phospholipid molecules, biological membrane fusion is a tightly controlled process that is mediated by a set of specialized proteins. In recent years, many of these proteins have been identified, although the exact role of them is still unknown. Three membrane proteins, each representing a small protein family conserved from yeast to humans, have emerged as key players in exocytotic and other intracellular fusion events (1–3). The variants involved in neuronal exocytosis are among the best characterized; they include the synaptic

vesicle protein synaptobrevin (also referred to as VAMP) and the synaptic membrane proteins SNAP-25¹ and syntaxin. Synaptobrevin and syntaxin are small integral membrane proteins with a single transmembrane domain at their respective C termini (4, 5), whereas SNAP-25 is anchored to the membrane by means of palmitoyl side chains attached to the middle of the molecule (6, 7). While the evidence is compelling that these proteins play a crucial role in membrane fusion, their mechanism of action is still controversial. Biological membrane fusion must ultimately be mediated by a series of ordered and reversible protein–protein interactions that are associated with conformational changes and that lead to a rearrangement of the phospholipid microenvironment. For these reasons, it is important to understand the structural rearrangements and the conformational states the fusion proteins assume during the fusion process. On the basis of a number of recent studies, a sketchy picture is emerging that assumes that an assembly–disassembly cycle is the basic

[†] This work was in part supported by grants from the National Institutes of Health to A.T.B. (GM54160-01) and to R.J. (NS33709-02). D.F. was supported by a grant from the Deutsche Forschungsgemeinschaft.

^{*} To whom correspondence should be sent: Department of Neurobiology, Max-Planck-Institute for Biophysical Chemistry, Am Fassberg 11, D-37077 Göttingen, Germany. Phone: x49-551-201-1634. Fax: x49-551-201-1639. E-mail: rjahn@gwdg.de.

[‡] Max-Planck-Institute for Biophysical Chemistry.

[§] Yale University.

¹ Abbreviations: NSF, *N*-ethylmaleimide sensitive fusion protein; SNAP, soluble NSF attachment protein; SNARE, SNAP receptors; SNAP-25, synaptosomal-associated protein of 25 kDa; BoNT, botulinum neurotoxin; TeNT, tetanus toxin; TCEP, tris(2-carboxyethyl)phosphine hydrochloride; CD, circular dichroism; NMR, nuclear magnetic resonance; MALLS, multiangle laser light scattering.

reaction underlying membrane fusion. First, all three proteins spontaneously assemble into a tight ternary complex with equimolar stoichiometry, regardless of whether these proteins are expressed in bacteria or purified from brain extracts (8, 9). Second, Rothman and co-workers found that the ATPase NSF (NEM-sensitive fusion protein), with the assistance of cofactors termed SNAPs, can reversibly disassemble the ternary complex into its individual constituents either in solution (8, 10) or in an intact membrane (11). NSF is therefore believed to be a member of a class of disassembly-promoting chaperones (12). Since SNAPs mediate the binding of NSF to the components of the ternary complex, these components are collectively termed SNARE (SNAP receptor) proteins (10).

It is generally accepted that the reversible assembly–disassembly reactions of the SNARE proteins are crucial for membrane fusion, but it is still unclear how fusion is mediated. Originally, it was proposed that assembly occurs during vesicle docking, resulting in an antiparallel complex, and that the rearrangement of the proteins during NSF-mediated disassembly drives the fusion reaction (1, 8). However, recent evidence has shown that the proteins are aligned parallel to their transmembrane anchors extending at one side of the complex (12, 13) and that NSF is probably not involved in the final steps of the fusion reaction (14–17). On the basis of these findings and on structural studies discussed further below (18–20), we have recently proposed an alternative model (3, 19). According to this view, the assembly reaction pulls together proteins of the two participating membranes. Assembly could proceed from the tips of the molecules toward their respective membrane anchor domains, forcing the membranes close together and thus overcoming the energy barrier for membrane fusion.

To differentiate between this and alternative hypotheses, it is important to understand the molecular details of the structural changes associated with the assembly reaction. We have therefore embarked on a detailed investigation of SNARE proteins and their complexes using a combination of molecular, biochemical, and biophysical techniques. The data available so far suggest that these proteins have highly unusual structural properties (18–20). First, both circular dichroism (CD) and nuclear magnetic resonance (NMR) spectroscopy revealed that of the three monomers only syntaxin shows significant secondary (α -helical) structure whereas SNAP-25, and particularly synaptobrevin, are unstructured (18, 19). Second, assembly into the synaptic ternary complex is associated with a dramatic increase in α -helical structure (19). Third, the ternary SNARE complex is thermally very stable, tolerating temperatures up to 80 °C without significant denaturation (19). Thus, assembly involves a change from largely unstructured synaptobrevin and SNAP-25 into a highly stable and structured complex. Interestingly, very similar features of the assembly reaction and of the resulting complex were found for a set of yeast homologues despite limited sequence similarities, indicating that these features are conserved and are essential hallmarks for the fusion reaction in yeast and humans (20).

In this study, we have used limited proteolysis of the ternary complex to identify the minimal domains sufficient for the assembly and disassembly of the core complex. Proteolysis resulted in a minimal complex that is fully competent for NSF-mediated disassembly. It consists of four

short polypeptides with molecular masses of about 10 kDa. Two of them comprise the C- and N-terminal half of SNAP-25, respectively; one contains almost the entire cytoplasmic domain of synaptobrevin, and one contains the C-terminal region of syntaxin.

EXPERIMENTAL PROCEDURES

Materials. NSF and α -SNAP in pQE-9 plasmids encoding His₆-tagged fusion proteins were kindly provided by S. Whiteheart and J. E. Rothman. The recombinant protein fragments were derived from cDNAs encoding rat synaptobrevin 2 and rat syntaxin 1A (kindly provided by R. H. Scheller) and for SNAP-25B (kindly provided by T. C. Südhof). The recombinant L chain of tetanus toxin (TeNT) was a generous gift of H. Niemann (Hannover, Germany).

Plasmid Construction. Subcloning was performed using standard techniques (21). For all polymerase chain reactions (PCRs), Pfu DNA polymerase was used. For bacterial expression, the cytoplasmic domain of rat synaptobrevin 2 (SB1–96) was subcloned into the pET-15b vector (Novagen), the cytoplasmic domain of rat syntaxin 1A (residues 1–265) into TrcHisA (Invitrogen), and full-length SNAP-25B (residues 1–206) into pHO2d (see ref 19 for details). For the generation of the protein fragments of the minimal core complex, we used PCR amplification followed by subcloning into the pET-15b vector (Novagen) which includes a thrombin cleavage site for the removal of the upstream tag. For the N-terminal half of SNAP-25B, the coding sequence for residues 1–83 (SN1) was amplified using the primers 5'-GCGCATATGGCCGAAGACGCGGATATG-3' and 5'-GCGCTCGAGTTATTTGCTAAATCTTTTAAATTTTTC-3'. The coding sequence for residues 120–206 (SN2) of SNAP-25B was amplified using the primers 5'-GCGCTC-GAGGTGGTGGATGAACGGGAG-3' and 5'-GCGGGATC-CCTACCCACTGCCAGCATC-3'. The coding sequence for residues 180–262 (SX180–262) of syntaxin was amplified using the primers 5'-GCGCATATGGGGATCATCATG-GACTCC-3' and 5'-GCGCTCGAGTTAGCGTGCCTTGC-TCTGGTA-3'. Subcloning of the SN1, SN2, and SX180–262 constructs into the pET-15b expression vector was performed using *Nde*I and *Xho*I (SN1 and SX180–262) and *Xho*I and *Bam*HI sites (SN2).

Protein Purification. All recombinant proteins were expressed as His₆-tagged fusion proteins and purified by Ni²⁺–Sephrose affinity chromatography. Proteins were eluted by increasing the imidazole concentration stepwise to 40, 80, 120, or 400 mM [in 20 mM Tris (pH 7.4) and 500 mM NaCl]. Fractions were analyzed for purity by SDS–PAGE and staining with Coomassie Blue. NSF was purified as described previously (12). Fractions containing recombinant proteins were dialyzed against standard buffer [20 mM Tris (pH 7.4), 1 mM EDTA, and 1 mM dithiothreitol (DTT)] containing 50 mM NaCl. During this step, the His₆ tags were cleaved by thrombin with the vector-derived residues Gly-Ser-His (SB1–96 and SN1), Gly-Ser-His-Met (SX180–262), or Gly-Ser-His-Met-Leu-Glu (SN2) remaining attached to the N terminus of the fragments.

All proteins were further purified by ion exchange chromatography using Mono-Q or Mono-S columns on an FPLC system (Pharmacia). After loading, the proteins were eluted with a linear gradient of NaCl in standard buffer. The peak

fractions were pooled and dialyzed against standard buffer containing 50 mM NaCl. The eluted proteins were 95% pure as determined by gel electrophoresis and mass spectrometry. The ternary (syntaxin–SNAP-25–synaptobrevin) complex and the recombinant minimal core complex consisting of SN1, SN2, SX180–262, and SB1–96 were purified using a Mono-Q column (Pharmacia) after overnight assembly of the purified monomers. The minimal core complex was further purified by size exclusion chromatography on a Superdex 200 HiLoad 16/60 prep grade column in standard buffer containing 300 mM NaCl at a flow rate of 1 mL/min. After purification, the proteins and the protein complexes were dialyzed against standard buffer and concentrated by ultrafiltration to final concentrations of 1–10 mg/mL. Protein concentrations, measured at 280 nm or/and the Bradford assay (22), were calibrated by internally standardized amino acid analysis following acid hydrolysis (carried out by the W. M. Keck Foundation Biotechnology Resource Laboratory at Yale University).

Limited Proteolysis. The purified ternary complex was subjected to limited protease digestions in standard buffer containing 100 mM NaCl using trypsin, chymotrypsin, and proteinase K, using a 1:100 (w:w) protease–protein complex at 25 °C. The reaction was stopped by adding PMSF containing SDS sample buffer and by placing the sample on ice. The digests were further analyzed by SDS–PAGE (23, 24).

Disassembly Reaction. The purified minimal core complex (5 μ M) was disassembled by addition of 1 μ M NSF, 12 μ M α -SNAP, 5 mM MgCl₂, and 1.5 mM ATP in standard buffer [20 mM Tris (pH 7.4), 1 mM EDTA, and 1 mM DTT] containing 100 mM NaCl for 1 h at 37 °C in the presence of 2 μ M TeNT light chain. The reaction was stopped by heating the samples for 5 min to 95 °C in SDS sample buffer. As controls, the reaction was carried out in the absence of NSF and/or α -SNAP, or the ATPase activity of NSF was abolished by replacing MgCl₂ with 10 mM EDTA. As an assay for disassembly (11), cleavage of synaptobrevin (SB1–96) by TeNT was monitored using tricine electrophoresis for fragment separation (24).

Characterization of the Components of the Protease-Resistant Core Complex. For purification of the protease-treated ternary complex, the complex was digested for 10 min at a 1:100 protease:ternary complex ratio with trypsin or proteinase K. Proteolysis was terminated by adding 10 mM PMSF. Size exclusion chromatography was then performed using a HR-10/30 Superdex 200 column (Pharmacia) in standard buffer containing 300 mM NaCl and 1 mM DTT at a flow rate of 0.5 mL/min. The fractions containing the protease-resistant complex were pooled and loaded on a Poros R1 column (Perseptive) using a high-performance liquid chromatography (HPLC) system (Rainin). The protein fragments were separated with a linear gradient from 0.12% TFA in water to 95% acetonitrile/0.1% TFA. The separated protein fragments were characterized by electrospray mass spectrometry (W. McMurray, Yale Medical School, Cancer Center, New Haven, CT) and peptide microsequencing (W. M. Keck Foundation Biotechnology Resource Laboratory at Yale University).

CD Spectroscopy. Far-UV CD spectra were obtained by averaging over 5–20 scans with a step size of 0.5 nm on an AVIV model 62DS CD spectrometer equipped with a

thermoelectric temperature controller. All measurements were performed in Hellma quartz cuvettes with path lengths between 0.1 and 0.2 cm. All CD spectra were recorded after reaching equilibrium following an overnight incubation at 4 °C in the buffer indicated in the panels. To evaluate changes of the CD spectrum that can be attributed to complex formation, the spectra were compared to the theoretically noninteracting sum of the individual spectra using the equation $[\Theta]_{\text{sum}} = \sum_i c_i n_i [\Theta]_i / \sum_i c_i n_i$, where c_i represents the respective concentrations of the proteins, n_i represents the respective numbers of amino acid residues, and $[\Theta]_i$ represents the mean residue ellipticities of the individual proteins. For thermal melts, the mean residue ellipticities at 220 nm were measured as a function of temperature.

Electrophoretic Procedures. Routinely, SDS–PAGE was carried out as described by Laemmli (23). When we tested for SDS resistance, samples were solubilized in SDS sample buffer [final concentrations of 60 mM Tris (pH 6.8), 2% SDS, 10% glycerol, and 3% β -mercaptoethanol] and incubated at room temperature (not boiled) or 95 °C (boiled) for 5 min before being analyzed on a 15% polyacrylamide gel. For analysis of the constituents of the protease-resistant core complex, tricine gel electrophoresis (16.5% T, 6% C) was used (24).

Nondenaturing gels were prepared and run in a manner identical to that of SDS–polyacrylamide gels except that SDS was omitted from all buffers. To allow for comparison with the spectroscopic data, the samples were incubated overnight in standard buffer at the concentrations indicated in the panels. After addition of sample buffer [final concentrations of 60 mM Tris (pH 6.8) and 10% glycerol], the samples were separated on a 3% stacking (Tris, pH 6.5) and a 9% separation gel (Tris, pH 8.8). All gels were stained with Coomassie Blue.

Multiangle Laser Light Scattering. Size exclusion chromatography was performed on a HR-10/30 Superdex 200 column (Pharmacia) in standard buffer with 300 mM NaCl and 10 mM TCEP at a flow rate of 0.5 mL/min. The elution profiles were monitored by UV absorption at 280 nm, light scattering at 690 nm, and differential refractometry. Light scattering and differential refractometry were carried out using the Mini-Dawn and Optilab instruments, respectively, of Wyatt Technology Corp. Analysis was carried out as described by Astra software (25). For each sample, 100 μ L of protein solution was loaded. The dn/dc value (change of solution refractive index with respect to a change in concentration of the molecules being investigated) is fairly constant for proteins (26) and was set to 0.185 for the analysis of the light scattering data.

Equilibrium Ultracentrifugation. Ultracentrifugation was performed at 21 and 40 °C using a Beckman Optima XL-I analytical ultracentrifuge in absorbance mode. Little difference was observed between the two temperatures. The protein sample was in 10 mM sodium phosphate (pH 7.5) and 150 mM NaCl. Three different concentrations (50, 36.5, and 18.5 μ M) in six sector cells were used to collect data at multiple speeds (10 000, 13 000, 16 000, 20 000, and 25 000 rpm). A partial specific volume of 0.75 mL/g was used. The solvent density was set to 1.0073 g/mL. Data sets were subjected to global analysis using the MICROCAL ORIGIN software (Beckman).

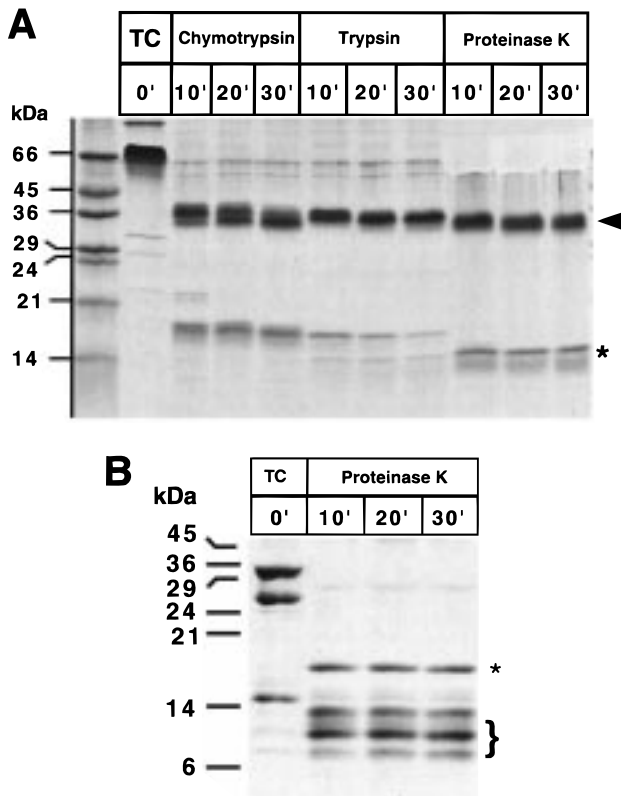


FIGURE 1: Limited proteolysis of the ternary synaptobrevin-SNAP-25-syntaxin complex gives rise to a SDS-resistant core complex. (A) Purified ternary complex (TC) was incubated with the three proteases chymotrypsin, trypsin, and proteinase K for the times (minutes) indicated. All samples were then analyzed by SDS-PAGE without boiling. Under these conditions, the purified ternary complex migrates as a single band at 67 kDa. Proteolysis resulted in a major band at 36–40 kDa (arrowhead) and smaller proteolytic fragments (asterisk). (B) The purified ternary complex was digested with proteinase K as in panel A, but this time, analysis was performed by tricine gel electrophoresis after boiling of the sample in SDS-containing sample buffer. As expected, the SDS-resistant ternary complex (TC) is dissociated into its constituent proteins. Note that the major band at 36–40 kDa disappeared and gave rise to several smaller bands (brace) in addition to the smaller proteolytic fragments (asterisk) seen also in panel A.

RESULTS

Identification of a Protease-Resistant Core Complex. To investigate whether the ternary complex of synaptobrevin, SNAP-25, and syntaxin contains a protease-resistant core, the ternary complex was assembled and purified as described (19) using bacterially expressed proteins that lack their membrane anchors. The purified ternary complex was then subjected to limited proteolysis using chymotrypsin, trypsin, and proteinase K. All digests were analyzed by SDS-PAGE without heating of the sample in SDS-containing sample buffer to investigate whether SDS resistance, a feature of the ternary complex (9), is preserved in the proteolysis products.

The ternary complex migrates as a single entity with an apparent molecular mass of about 67 kDa (Figure 1A, first lane), consistent with previous results (9, 12, 19). Proteolysis with each of the three proteases yielded a single major band with an apparent molecular mass of around 36–40 kDa that was stable even during prolonged incubation (Figure 1A, arrowhead). Furthermore, smaller fragments in the molecular mass range of 15–18 kDa emerged (Figure 1A, asterisk).

These smaller fragments are amino-terminal fragments of syntaxin as determined by N-terminal sequencing (data not shown). Heating of the sample in SDS-containing sample buffer resulted in the disappearance of the major 40 kDa protein band and the appearance of smaller fragments in the molecular mass range of 6–14 kDa (Figure 1B). The 18 kDa N-terminal fragments of syntaxin were not affected by heating (Figure 1B, asterisk). Thus, proteolysis of the ternary complex generated a SDS-resistant 40 kDa “minimal” complex. Since the results were similar for all three proteases, we restricted further analysis to the minimal complexes generated by trypsin and proteinase K digestion.

As a first step, the minimal complex generated by the protease digests was separated from other proteolytic fragments by size exclusion chromatography. The purified complexes were then denatured in trifluoroacetic acid, and the peptide constituents were separated using reversed phase HPLC. The components of the minimal complex eluted as well separated peaks (not shown) which were subsequently analyzed by amino-terminal sequencing and electrospray mass spectrometry. The results are summarized in Figure 2.

As expected, fragments derived from all three constituents of the full-length ternary complex were identified. Synaptobrevin was least affected by proteolysis. Proteinase K generated two fragments that lacked four and six N-terminal residues, respectively, but did not cleave at the C terminus of synaptobrevin. Trypsin cleaved only the last two C-terminal residues of the construct. In contrast, syntaxin was cleaved internally, resulting in the removal of the N-terminal two-thirds of the molecule from the SDS-resistant core complex. The C-terminal fragments produced by trypsin extended from residue 159 to either residue 260 or 262. Proteinase K treatment yielded two shorter fragments consisting of residues 180–262 and 184–262. The difference between the two digests can be explained by a lack of tryptic cleavage sites downstream of residue 159. Interestingly, the N terminus of the proteinase K product extends a few residues beyond the region described previously as the H3 domain (residues 191–266) (27). Analysis of the fragments derived from SNAP-25 revealed that both proteases excised the middle region which contains the putative membrane anchor domain. The resulting N- and C-terminal fragments remained in the SDS-resistant core complex. The N-terminal fragments generated by the two proteases were identical (residues 2–83). The C-terminal fragments generated by trypsin extended from residues 120 or 125 to the C-terminal end of the SNAP-25 construct, including the entire His₆ tag. Proteinase K generated a very similar fragment beginning at residue 115 and including some residues of the C-terminal His₆ tag. These findings highlight the importance of the C-terminal end of SNAP-25, whose cleavage by botulin neurotoxins is associated with severe impairment of exocytosis.

Complexes Formed between Individual Components of the Minimal Core Complex. To further study the properties of the protease-resistant core complex, the following fragments were recombinantly expressed as His₆ tag proteins in *Escherichia coli*: syntaxin, residues 180–262; SNAP-25, residues 1–83 and 120–206; and synaptobrevin, residues 1–96 (i.e., unchanged). The proteins were purified, and the affinity tag was removed by thrombin cleavage, leaving three

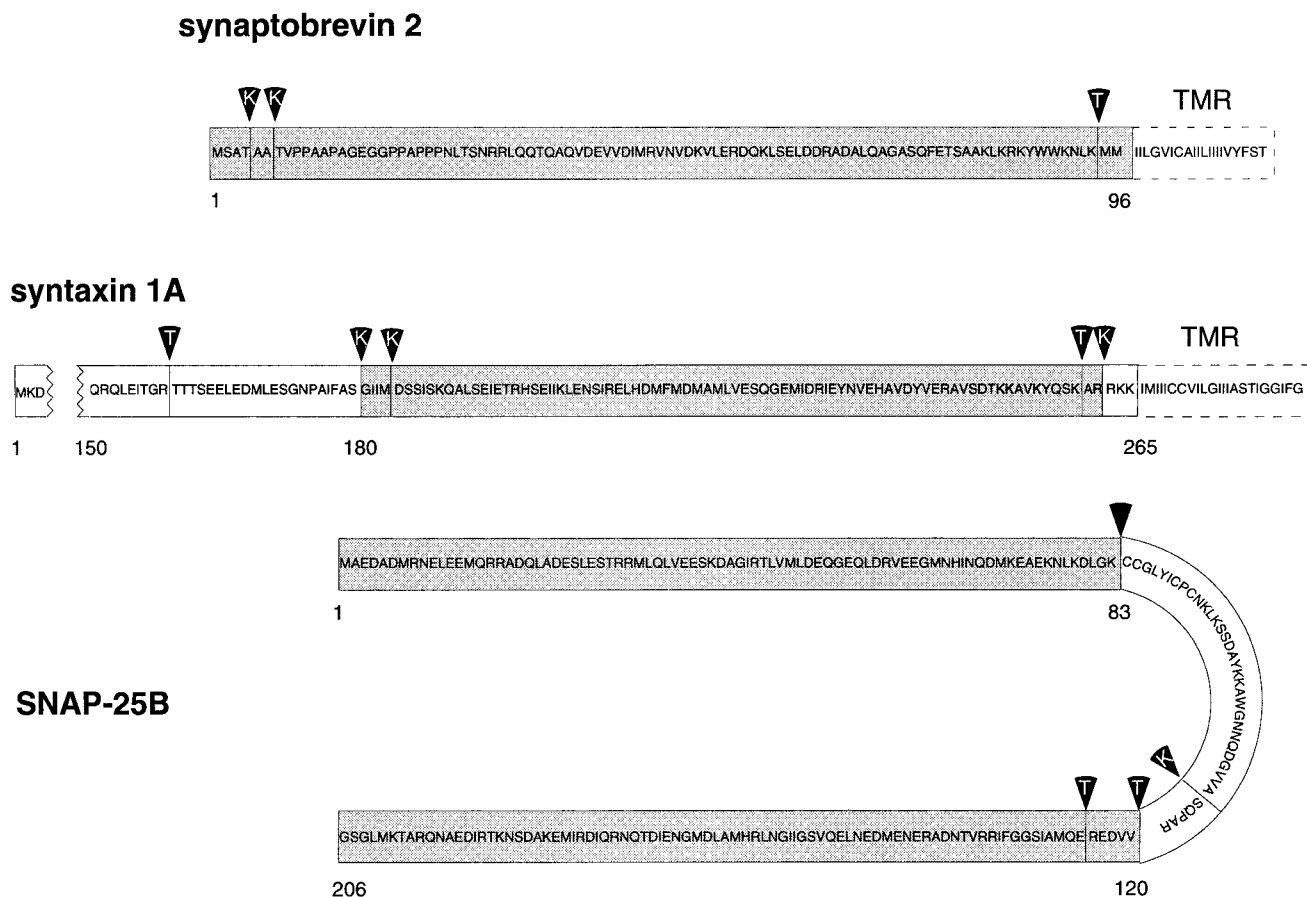


FIGURE 2: Schematic representation of the fragments obtained by limited protease digestion using trypsin or proteinase K. The components of the ternary complex, synaptobrevin, SNAP-25, and the C-terminal part of syntaxin, are depicted with the amino acid sequence in single-letter code. The cysteine-rich domain of SNAP-25 which is anchored to the membrane by means of palmitoyl side chains is drawn as a loop. The transmembrane regions of synaptobrevin and syntaxin are included (dotted lines) but were not part of the recombinant ternary complex subjected to limited proteolysis. Arrows (T, trypsin; K, proteinase K; or both) indicate the predominant cleavage sites of the respective proteases as determined by N-terminal sequencing and mass spectrometry. The gray shaded regions correspond to the fragments that were generated by bacterial expression for a more detailed analysis.

to six additional residues attached to the N terminus (see Experimental Procedures). The synaptobrevin and both SNAP-25 fragments were monomeric, whereas the syntaxin fragment appeared to be trimeric as determined by multiangle laser light scattering (MALLS, not shown).

CD spectroscopy revealed that only the syntaxin fragment had significant α -helical content, consistent with previous results (28). Synaptobrevin and both SNAP-25 fragments were largely unstructured, similar to previous results (not shown; see refs 18 and 19). Furthermore, the syntaxin fragment formed stable complexes either with the N-terminal or with both fragments of SNAP-25 but not with the C-terminal fragment alone (Figure 4, lanes 9 and 10), again consistent with previous results (18). Formation of these subcomplexes was associated with an increase in α -helical content that was more pronounced than that observed previously for the full-length proteins (Figure 3, columns 13–15; see ref 18). In contrast to uncleaved syntaxin, a slight increase in α -helical content was observed when the syntaxin fragment was combined with synaptobrevin (Figure 3, column 5), although no complex was observed in nondenaturing gels (not shown). It was previously suggested that the N-terminal portion of syntaxin might prevent the binding of synaptobrevin (29) which would explain this observation.

Interestingly, synaptobrevin was able to form stable subcomplexes with syntaxin when either the N- or C-terminal domain of SNAP-25 was present (Figure 3, columns 10 and 11, and Figure 4, lanes 5 and 6), whereas it does not interact with the individual or combined SNAP-25 fragments alone (Figure 3, columns 6, 7, and 9; see also ref 19). Formation of these subcomplexes is associated with a major increase in α -helical content (Figure 3, columns 10 and 11). Furthermore, synaptobrevin in these complexes was resistant to proteolytic cleavage by the tetanus toxin (TeNT) light chain (not shown).

When all four fragments were combined, a complex was formed (Figure 4, lanes 7 and 8) that was again accompanied by a pronounced increase in α -helical content (Figure 3, column 12). This reassembled minimal complex was resistant to SDS treatment, suggesting that it corresponds to the minimal complex generated by proteolysis. In contrast, the subcomplexes containing only one of the two SNAP-25 fragments were not SDS-resistant (not shown).

Structural and Functional Properties of the Minimal Complex. The properties of the purified minimal complex containing all four fragments were as remarkable as those of the full-length ternary complex. On the basis of its molar ellipticity (Figure 5A), its α -helical content was calculated to be about 58% (50% for the full-length ternary complex;

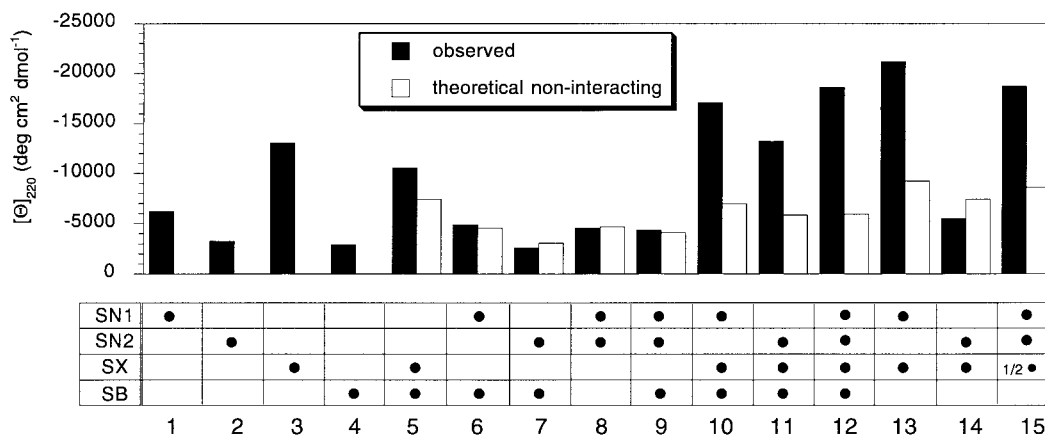


FIGURE 3: Changes in the mean residue ellipticity $[\Theta]$ at 220 nm induced by interaction between the components of the protease-resistant core complex. CD spectra were recorded in standard buffer containing 100 mM NaCl at 25 °C. White columns represent the theoretically noninteracting mean residue ellipticities at 220 nm calculated from the observed CD spectra of the individual proteins (columns 1–4). To obtain the spectra of the various combinations (black columns), the proteins were incubated overnight at 4 °C using about equimolar ratios (exception, column 15 since the syntaxin–SNAP-25 complex has a 2:1 stoichiometry; 19). The following concentrations were used: SN1 (6 μ M), SN2 (6 μ M), SB1–96 (5.1 μ M), and SX180–262 [4.8 μ M, except for the mix with SN1 and SN2 (column 15) where 2.4 μ M was used].

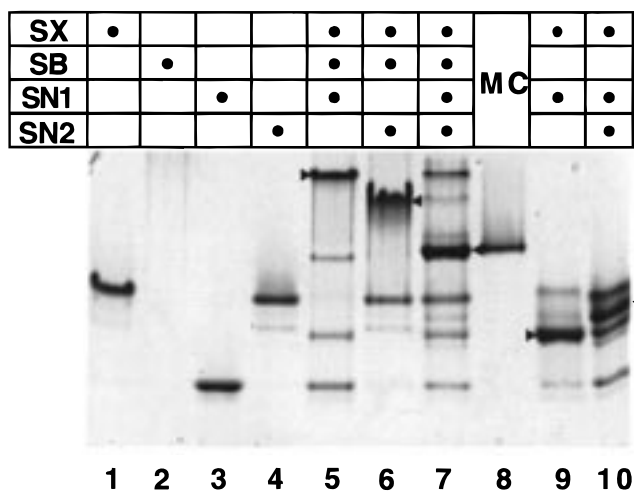


FIGURE 4: Complex formation between the components of the protease-resistant core, analyzed by nondenaturing gel electrophoresis and visualized by Coomassie Blue staining. All incubations were performed as described in the legend of Figure 3. Note that synaptobrevin is not detectable in the nondenaturing gel (lane 2) due to its isoelectric point of 8.5. In lanes 5–10, arrowheads indicate the position of major bands that do not correspond to any of the monomers and reflect complexes. In lane 8, the purified minimal complex (MC) was used.

see ref 19) and the complex was virtually resistant to heat denaturation up to 95 °C (Figure 5B).

Furthermore, we investigated whether the complex exists as a monomeric particle or whether it forms higher-order oligomers. Oligomerization may be important during membrane fusion since it can be expected that single monomers are not sufficient to drive the fusion reaction. The minimal complex eluted as a single peak from a size exclusion column. Analysis by MALLS, however, revealed an apparent concentration-dependent molecular mass in the range of 60–97 kDa (not shown), which suggests oligomerization of the 41 kDa monomer. To investigate the association state of the minimal complex in more detail, we performed analytical equilibrium ultracentrifugation. A good fit was achieved with a monomer–trimer equilibrium ($K_D \approx 3 \mu$ M) (Figure 6) using three speeds and two different concentra-

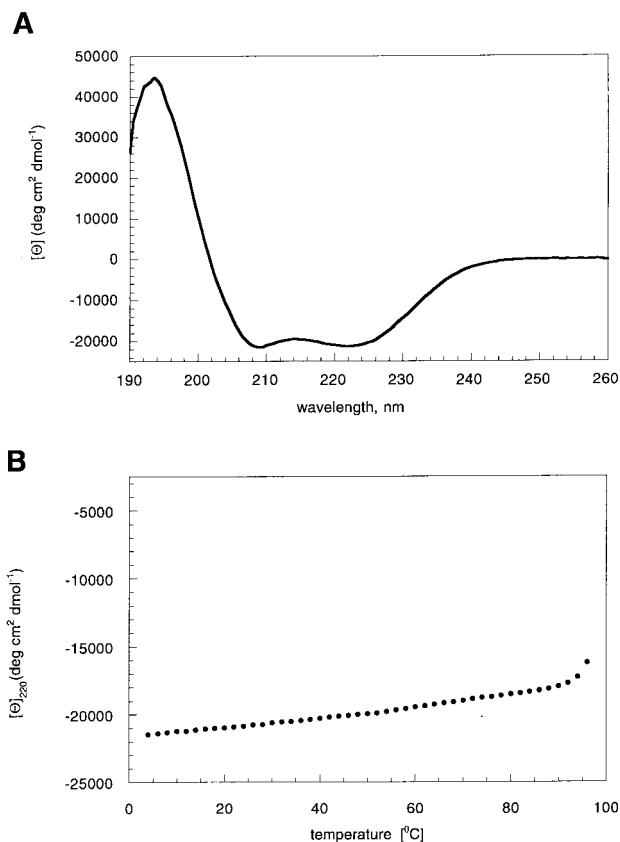


FIGURE 5: CD spectrum and thermal stability of the protease-resistant core complex. (A) CD spectrum of the purified minimal core complex (30.9 μ M) at 25 °C in 20 mM sodium phosphate (pH 7.5) containing 50 mM NaCl. (B) Change in the mean residue ellipticity $[\Theta]$ at 220 nm of the purified minimal core complex (30.9 μ M) in standard buffer containing 100 mM NaCl as a function of temperature. The temperature increment was 2 °C, the equilibration time 3 min, and the averaging time 1 min.

tions. It should be noted, however, that data obtained at higher speeds and at lower concentrations could not be fitted to a unique model, suggesting the presence of smaller subcomplexes at low concentrations (not shown). In all the models used for fitting, no higher oligomeric species emerged (Figure 6).

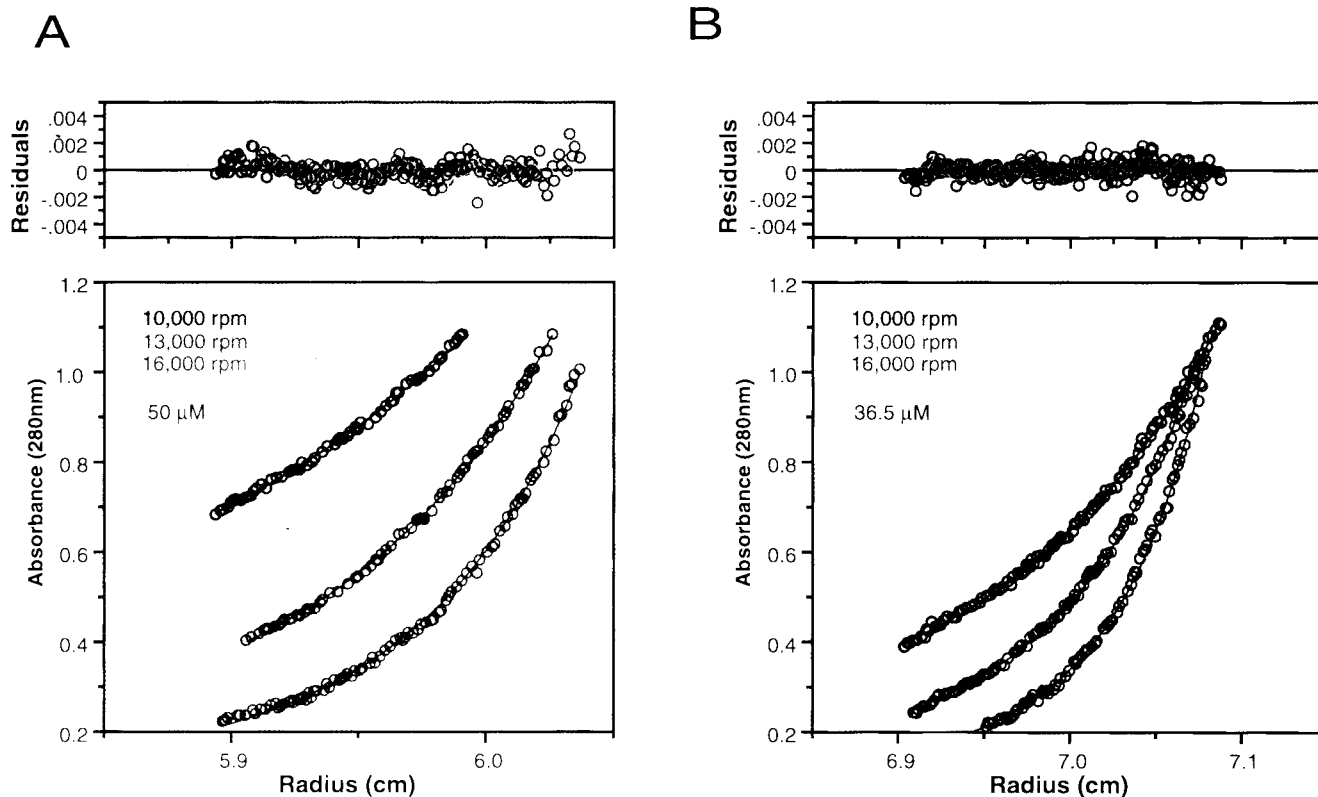


FIGURE 6: Determination of the oligomeric state of the minimal complex. Sedimentation equilibrium data and residuals at a concentration of 50 μM (A) and 36.5 μM (B) using rotor speeds of 10 000 (blue circles), 13 000 (green circles), and 16 000 (red circles) rpm. Solid lines show a global fit to a monomer-trimer equilibrium, where the monomer is assumed to be a 1:1:1:1 (SX180-262-SB1-96-SN1-SN2) complex of 41 kDa. The global fit was performed using the data shown. The goodness of the fit was 0.378 (χ^2 of the nonlinear fit).

Finally, we investigated whether the minimal core complex can be disassembled by the action of the ATPase NSF in conjunction with α -SNAP. As an assay for disassembly, we used the susceptibility of synaptobrevin to cleavage by the TeNT light chain. Previous work has shown that the constituents of the ternary complex are resistant to the action of clostridial neurotoxins but become susceptible to cleavage upon disassembly (9, 11, 30, 31). Incubation of the complex with purified NSF and α -SNAP in the presence of Mg-ATP rendered synaptobrevin susceptible to cleavage by the TeNT light chain (Figure 7). Thus, the fragments present in the minimal core complex not only contain the domains essential for assembly but also are sufficient for disassembly by NSF and α -SNAP.

DISCUSSION

In this study, we have used limited proteolysis as a tool to excise a core domain of the neuronal SNARE complex which is sufficient for its reversible assembly and disassembly. Our data identify this minimal core complex as a defined structural entity that is capable of carrying out complete assembly and disassembly reactions. The structural changes occurring during assembly and the biophysical properties of the fully assembled complex are remarkable and suggest once again a link between these properties and the role of the SNARE proteins in the fusion machine which is conserved during evolution. The major features of the assembly reaction are consistent with our recently proposed model of membrane fusion. This model implies that the assembly reaction of SNARE proteins generates an attractive

force between membranes which brings them into close apposition, thus promoting membrane fusion (3, 12, 19, 20).

Proteolytic mapping of the core domains resulted in fragments that are similar to interacting domains identified by deletion mutagenesis (9, 27-29, 32, 33). Our study produced several interesting new insights. First, the excision of the cysteine-rich loop in SNAP-25 thought to carry the palmitoyl side chains shows that this domain does not participate in complex formation. The observation lends further support to the view that this region serves as a membrane anchor domain. Second, our data confirm that the C-terminal H3 domain of syntaxin is necessary and sufficient for complex formation and disassembly. This domain appears to function as a "nucleation site" for the entire complex since no stable associations can be formed without its participation. Third, all domains left intact by the proteases (including proteinase K, a voracious and nonspecific enzyme that disrespects even membrane barriers) include the cleavage sites for clostridial neurotoxins and are larger than the sites inferred from studies using deletion mutagenesis or toxin cleavage products. In fact, it is possible to assemble complexes from smaller fragments, for instance, fragments generated by toxin cleavage. Some of these complexes are stable in SDS (31, 33, 34). However, resistance to proteolysis indicates that these additional amino acids belong to structurally defined entities and thus are an integral part of the core domain.

Our data further show that the minimal core complex can be disassembled by α -SNAP and NSF. This is not surprising since incomplete complexes (35) or complexes composed

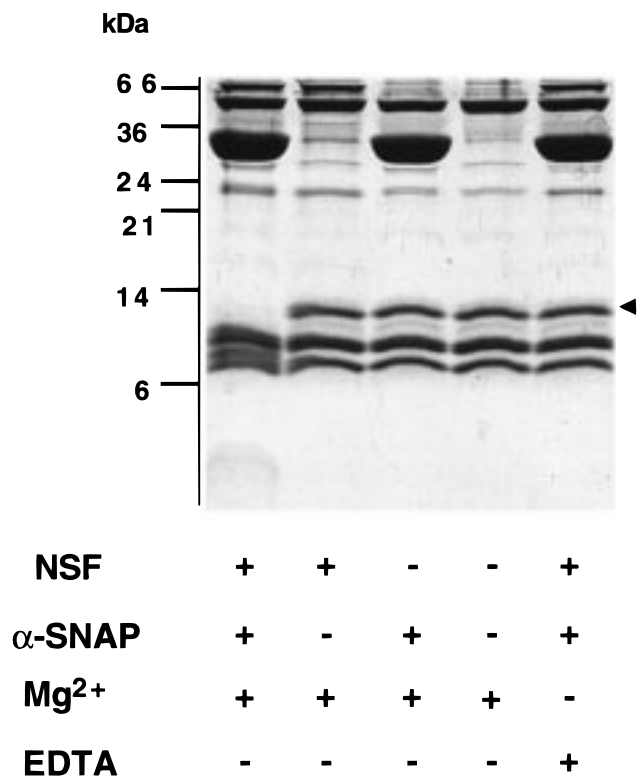


FIGURE 7: Disassembly of the protease-resistant core complex. The purified minimal core complex (5 μ M) was incubated as indicated in the panels in the presence of 1.5 mM ATP and 2 μ M TeNT light chain in standard buffer containing 100 mM NaCl for 1 h at 37 °C. NSF-driven disassembly rendered synaptobrevin susceptible to cleavage by the TeNT light chain that was monitored by tricine gel electrophoresis. The uncleaved SB1-96 band is indicated by an arrowhead.

of toxin-generated fragments (31, 34, 36) can be acted upon by these disassembly chaperones. Furthermore, all previously characterized binding sites for α -SNAP are contained in the minimal core complex (34, 35, 37). It should be mentioned that we and others were previously unable to measure disassembly in complexes containing N-terminally truncated syntaxin (34, 35). In those experiments, however, rapid reassembly following disassembly could not be observed, whereas in our approach, disassembly was monitored by immediate cleavage of synaptobrevin monomers released from the complex.

Obviously, high-resolution structural information is required before the precise alignment of the proteins will be known. However, our findings suggest that the minimal SNARE complex consists of an assembly of four highly α -helical peptides. In this context it is interesting to note that the binary complex between syntaxin and SNAP-25 has a 2:1 stoichiometry and exhibits features similar to, albeit less pronounced than, those of the ternary complex. Possibly, the position of synaptobrevin is occupied by the second syntaxin molecule in this complex (19). This may explain why in some systems residual fusion activity is observed in the absence of v-SNAREs (16, 38–40); t-SNAREs alone may be capable of forming complexes that pull membranes together, although less tightly than the ternary complex.

We observed that complexes can be formed with only one arm of the two-pronged SNAP-25 molecule. These findings suggest that the two halves of the molecule may act rather independently in their respective protein–protein interactions.

One could speculate that in the plane of the membrane the assembled “ternary” complexes could contain the C-terminal domain of one and the N-terminal domain of a second SNAP-25 molecule, opening the possibility for the formation of linear or circular oligomers. Indeed, the surprisingly high fraction of SDS-resistant higher-order complexes in native membranes (11) and also some of the higher-order complexes observed in vitro (20) may represent such oligomeric forms. It is exceedingly important to learn more about the formation of such oligomeric structures and their potential regulation. Membrane fusion is likely to require the assembly of multiple copies of ternary complexes in ring-shaped higher-order structures for the initialization of a fusion pore opening.

ACKNOWLEDGMENT

We thank Dieter Bruns, Klaus Fiebig, Martin Margittai, Rainer Ossig, Christian Ostermeyer, Henning Otto, Luke M. Rice, R. Bryan Sutton, and Richard Yu for stimulating discussions, Michael Ibba for critical reading of the manuscript, W. McMurray (Yale Medical School, Cancer Center, New Haven, CT) for help with the mass spectrometry, and Myron Crawford (W. M. Keck Foundation Biotechnology Resource Laboratory at Yale University) for help with the N-terminal sequencing and amino acid analysis.

NOTE ADDED IN PROOF

After submission of this paper, a protease-resistant core complex was also described by another group (41).

REFERENCES

- Rothman, J. E. (1994) *Adv. Second Messenger Phosphoprotein Res.* 29, 81–96.
- Calakos, N., and Scheller, R. H. (1996) *Physiol. Rev.* 76, 1–29.
- Hanson, P. I., Heuser, J. E., and Jahn, R. (1997) *Curr. Opin. Neurobiol.* 7, 310–315.
- Südhof, T. C. (1995) *Nature* 375, 645–653.
- Bennett, M. K., Calakos, N., and Scheller, R. H. (1992) *Science* 257, 255–259.
- Hess, D. T., Slater, T. M., Wilson, M. C., and Skene, J. H. P. (1992) *J. Neurosci.* 12, 4634–4641.
- Veit, M., Söllner, T. H., and Rothman, J. E. (1996) *FEBS Lett.* 385, 119–123.
- Söllner, T., Bennett, M. K., Whiteheart, S. W., Scheller, R. H., and Rothman, J. E. (1993) *Cell* 75, 409–418.
- Hayashi, T., McMahon, H., Yamasaki, S., Binz, T., Hata, Y., Südhof, T. C., and Niemann, H. (1994) *EMBO J.* 13, 5051–5061.
- Söllner, T., Whiteheart, S. W., Brunner, M., Erdjument-Bromage, H., Geromanos, S., Tempst, P., and Rothman, J. E. (1993) *Nature* 362, 318–324.
- Otto, H., Hanson, P. I., and Jahn, R. (1997) *Proc. Natl. Acad. Sci. U.S.A.* 94, 6197–6201.
- Hanson, P. I., Roth, R., Morisaki, H., Jahn, R., and Heuser, J. E. (1997) *Cell* 90, 523–535.
- Lin, R. C., and Scheller, R. H. (1997) *Neuron* 19, 1087–1094.
- Mayer, A., Wickner, W., and Haas, A. (1996) *Cell* 85, 83–94.
- Mayer, A., and Wickner, W. (1997) *J. Cell Biol.* 136, 307–317.
- Nichols, B. J., Ungermann, C., Pelham, H. R., Wickner, W. T., and Haas, A. (1997) *Nature* 387, 199–202.
- Ungermann, C., Nichols, B. J., Pelham, H. R., and Wickner, W. (1998) *J. Cell Biol.* 140, 61–69.
- Fasshauer, D., Bruns, D., Shen, B., Jahn, R., and Brünger, A. T. (1997) *J. Biol. Chem.* 272, 4582–4590.
- Fasshauer, D., Otto, H., Eliason, W. K., Jahn, R., and Brünger, A. T. (1997) *J. Biol. Chem.* 272, 28036–28041.

20. Rice, L. M., Brennwald, P., and Brünger, A. T. (1997) *FEBS Lett.* 415, 49–55.
21. Saiki, R. K., Gelfand, D. H., Stoffel, S., Scharf, S. J., Higuchi, R., Horn, G. T., Mullis, K. B., and Ehrlich, H. A. (1988) *Science* 239, 487–491.
22. Bradford, M. M. (1976) *Anal. Biochem.* 72, 248–254.
23. Laemmli, U. K. (1970) *Nature* 227, 680–685.
24. Schägger, H., and von Jagow, G. (1987) *Anal. Biochem.* 166, 368–379.
25. Wyatt, P. (1993) *Anal. Chim. Acta* 272, 1–40.
26. Wen, J., Arakawa, T., and Philo, J. S. (1996) *Anal. Biochem.* 240, 155–166.
27. Kee, Y., Lin, R. C., Hsu, S. C., and Scheller, R. H. (1995) *Neuron* 14, 991–998.
28. Zhong, P., Chen, Y. A., Tam, D., Chung, D., Scheller, R. H., and Miljanich, G. P. (1997) *Biochemistry* 36, 4317–4326.
29. Calakos, N., Bennett, M. K., Peterson, K. E., and Scheller, R. H. (1994) *Science* 263, 1146–1149.
30. Pellegrini, L. L., O'Connor, V., and Betz, H. (1994) *FEBS Lett.* 353, 319–323.
31. Pellegrini, L. L., O'Connor, V., Lottspeich, F., and Betz, H. (1995) *EMBO J.* 14, 4705–4713.
32. Chapman, E. R., An, S., Barton, N., and Jahn, R. (1994) *J. Biol. Chem.* 269, 27427–27432.
33. Hao, J. C., Salem, N., Peng, X. R., Kelly, R. B., and Bennett, M. K. (1997) *J. Neurosci.* 17, 1596–1603.
34. Hayashi, T., Yamasaki, S., Nauenburg, S., Binz, T., and Niemann, H. (1995) *EMBO J.* 14, 2317–2325.
35. Hanson, P. I., Otto, H., Barton, N., and Jahn, R. (1995) *J. Biol. Chem.* 270, 16955–16961.
36. Otto, H., Hanson, P. I., Chapman, E. R., Blasi, J., and Jahn, R. (1995) *Biochem. Biophys. Res. Commun.* 212, 945–952.
37. McMahon, H. T., and Südhof, T. C. (1995) *J. Biol. Chem.* 270, 2213–2217.
38. Broadie, K., Prokop, A., Bellen, H. J., O'Kane, C. J., Schulze, K. L., and Sweeney, S. T. (1995) *Neuron* 15, 663–673.
39. Sweeney, S. T., Broadie, K., Keane, J., Niemann, H., and O'Kane, C. J. (1995) *Neuron* 14, 341–351.
40. Deitcher, D. L., Ueda, A., Stewart, B. A., Burgess, R. W., Kidokoro, Y., and Schwarz, T. L. (1998) *J. Neurosci.* 18, 2028–2039.
41. Poirier, M. A., et al. (1998) *J. Biol. Chem.* 273, 11370–11377.

BI980542H